Lipids (2015) 50:821–836
DOI 10.1007/s11745-015-4044-6

METHODS

Characterization of Wax Esters by Electrospray Ionization Tandem Mass Spectrometry: Double Bond Effect and Unusual Product Ions

Jianzhong Chen[1,2,3] · **Kari B. Green**[2,4] · **Kelly K. Nichols**[5,3]

Received: 24 October 2014 / Accepted: 22 June 2015 / Published online: 16 July 2015

Abstract A series of different types of wax esters (represented by RCOOR′) were systematically studied by using electrospray ionization (ESI) collision-induced dissociation tandem mass spectrometry (MS/MS) along with pseudo MS^3 (in-source dissociation combined with MS/MS) on a quadrupole time-of-flight (Q-TOF) mass spectrometer. The tandem mass spectra patterns resulting from dissociation of ammonium/proton adducts of these wax esters were influenced by the wax ester type and the collision energy applied. The product ions $[RCOOH_2]^+$, $[RCO]^+$ and $[RCO-H_2O]^+$ that have been reported previously were detected; however, different primary product ions were demonstrated for the three wax ester types including: (1) $[RCOOH_2]^+$ for saturated wax esters, (2) $[RCOOH_2]^+$, $[RCO]^+$ and $[RCO-H_2O]^+$ for unsaturated wax esters containing only one double bond in the fatty acid moiety or with one additional double bond in the fatty alcohol moiety, and (3) $[RCOOH_2]^+$ and $[RCO]^+$ for unsaturated wax esters containing a double bond in the fatty alcohol moiety alone. Other fragments included $[R']^+$ and several series of product ions for all types of wax esters. Interestingly, unusual product ions were detected, such as neutral molecule (including water, methanol and ammonia) adducts of $[RCOOH_2]^+$ ions for all types of wax esters and $[R'-2H]^+$ ions for unsaturated fatty acyl-containing wax esters. The patterns of tandem mass spectra for different types of wax esters will inform future identification and quantification approaches of wax esters in biological samples as supported by a preliminary study of quantification of isomeric wax esters in human meibomian gland secretions.

Keywords Wax esters · Mass spectrometry · Electrospray ionization · Fragmentation · Double bond · Neutral molecule adducts

Abbreviations

APCI	Atmospheric pressure chemical ionization
CI	Chemical ionization
CID	Collision induced dissociation
EI	Electron ionization
ESI	Electrospray ionization
MRM	Multiple-reaction monitoring
MS/MS	Tandem mass spectrometry
MS^3 (MS/MS/MS)	Multi-stage tandem mass spectrometry
Pseudo MS^3	In source dissociation combined with MS/MS
Q-TOF	Quadrupole time-of-flight

Introduction

Wax esters are the esters of long chain fatty acids and fatty alcohols, which are conventionally represented by

Electronic supplementary material The online version of this article (doi:10.1007/s11745-015-4044-6) contains supplementary material, which is available to authorized users.

✉ Jianzhong Chen
jzchen@uab.edu

1 Applied Biotechnology Branch, Air Force Research Laboratory, Dayton, OH 45433, USA

2 Mass Spectrometry and Proteomics Facility, The Ohio State University, Columbus, OH 43210, USA

3 Present Address: School of Optometry, The University of Alabama at Birmingham, Birmingham, AL 35294-0010, USA

4 Present Address: Department of Chemistry, University of Florida, Gainesville, FL 32611, USA

5 College of Optometry, University of Houston, Houston, TX 77204, USA

RCOOR′, where R and R′ are the alkyl moieties of fatty acid and fatty alcohol, respectively. They are an abundant component in beeswax [1], marine organism waxes [2], plant surface waxes [3], insect surface waxes [4], skin lipids [5] and meibomian gland secretions (meibum) [6, 7]. The functions of wax esters include storing energy, providing buoyancy and insulation, and preventing water loss.

Previously, wax esters were primarily detected and identified by mass spectrometry using electron ionization (EI) [8–12] and chemical ionization (CI) [13]. Recently, a relatively new ionization mode—atmospheric pressure chemical ionization (APCI), has also been applied to the analysis of wax esters [14, 15]. However, these ionization modes are energetic, which leads to in-source dissociation of wax esters and other labile lipids such as cholesteryl esters [16], complicating the identification and quantification of lipid compositions in samples.

Electrospray ionization (ESI), a softer ionization mode, has been increasingly utilized for detection of wax esters [17, 18] and other types of lipids [19]. It has the advantage of negligible in-source dissociation of ions during MS analysis, enabling more reliable quantitation studies and simultaneous detection of different classes of intact lipids in biological samples such as wax esters in meibum [6, 20]. However, wax esters, a type of neutral lipid lacking polar groups for cation adduct formation, are generally more difficult to detect with ESI–MS [21] and thus are often overlooked in lipidomic analysis of biological samples. Nevertheless, recent reports show that wax esters can be readily detected using additives such as ammonium acetate [6, 17], ammonium formate [20], lithium acetate [18], sodium acetate [6] or trifluoroacetic acid [22].

The CID spectra of wax esters using ESI [17, 20, 23–25], CI [13] and APCI [15] have been reported and the major product ions have been applied for identification and quantitation of wax esters. Some of these studies utilized a method known as multiple-reaction monitoring (MRM) [26] in which only one or very few product/precursor ion pairs (or transition) were used for detection and quantification of specific wax esters in complex biological samples such as seed oils and meibomian gland secretions [23–25]. This MRM approach negates the need for scanning resulting in increased detection sensitivity and greater analysis throughput. However, this technique has a high probability of false detection of impurity ions as the intended targeted ions, as recently emphasized by the proteomics field [27]. The false detection problem is compounded for wax esters as they are often more difficult to ionize than many common contaminants [28]. Therefore, obtaining more detailed information on the dissociation patterns of wax esters under various conditions will help avoid false positive detection.

In this work, CID was performed on a set of saturated and unsaturated wax ester standards with the double bond(s) located in either or both moieties of the wax esters. The dissociation patterns of wax esters varied depending on the type of wax esters and the collision energies. In addition to the commonly reported product ions, many other novel product ions were detected expanding our understanding of wax ester dissociation pathways and suggesting that great care must be taken when using the MRM technique for quantitation of wax esters.

Experimental

Chemicals

Sodium iodide (>99.999 %), chloroform (HPLC grade, >99.9 %, with amylene as the stabilizer, either Burdick & Jackson or Sigma brand), methanol (HPLC grade, >99.9 %, Riedel-de Haen), and ammonium acetate (>98 %, Sigma) were purchased from Sigma-Aldrich (St. Louis, MO). Ten wax ester standards, namely, behenyl palmitate, behenyl stearate, palmityl behenate, behenyl palmitoleate, behenyl oleate, arachidyl oleate, stearyl oleate, oleyl stearate, palmitoleyl behenate, and oleyl oleate were purchased from Nu-Chek Prep (Elysian, MN) and Sigma-Aldrich (St. Louis, MO).

Electrospray Time-of-Flight Mass Spectrometry Analysis

A Quadrupole Time-of-Flight mass spectrometer (Q-TOF II; Waters, Milford, MA) was used for all analyses. The stock standard solutions were prepared by individually dissolving 2.1–24 mg of wax ester standard into 1 mL chloroform/methanol mixture (2:1 by volume). The working solutions were prepared by diluting the stock solutions 100 or 1000 fold using chloroform/methanol mixture (2:1 by volume) that contained 1 % water and 1 mM ammonium acetate additive; final concentrations of wax ester standards were 25–53 μM. Meibum sample collection and solution preparation has been described previously [6, 29]. Briefly, meibum was collected in 0.5-μL (32 mm length, 0.0220″ OD, 0.00560″ ID) glass microcapillary tubes (Drummond, Broomall, PA) with a length of about 1 mm, and was then dissolved in chloroform–methanol solvent mixture (2:1 vol/vol) with a concentration of approximately 6.7 μg/mL of total lipids and 1 mM ammonium acetate additive.

The working solutions were directly infused into the mass spectrometer at a flow rate of 10–20 μL/min. The detection was in positive mode; the cone voltage was set at 15 V (for MS analysis of wax esters and MS/MS analysis of ammoniated wax esters) or 50 V (for MS/MS analysis of protonated and sodiated wax esters); the source and desolvation temperatures were set at 100 and 150 °C, respectively; the capillary voltage was set at 3 kV. The instrument was calibrated using sodium iodide cluster ions. After calibration, the sodium iodide in the system was thoroughly cleaned to minimize sodiated adduct formation (a

trace amount of sodium ions in solvents and glassware is always present). MS analysis was performed using a collision energy of 5 eV to increase ion transmission in the absence of significant fragmentation. MS/MS analysis was performed with collision-induced dissociation (CID) of the isolated peaks of interest; high mass and low mass resolutions were set at 15; the collision energies were set at 5, 10, 20 or 30 eV. The acquisition time was typically less than 1 min. Pseudo MS^3 analysis [30, 31], i.e., combining in-source dissociation and MS/MS analysis, was performed to confirm assignment of some of the product ion peaks; in-source dissociation was achieved by raising the cone voltage from 15 to 50 V.

Assignments of Peaks in MS/MS Spectra

For the MS/MS spectra of these wax ester standards, the peaks corresponding to $[RCOOH_2]^+$, $[R']^+$, $[RCO]^+$, $[M+H]^+$, and $[M+NH_4]^+$ were assigned with high confidence. Additional peaks, particularly those at low *m/z* regions, were assigned by using the "elemental composition" program in MassLynx (Waters, Milford, MA). The spectra were calibrated by a single point lock mass correction using $[RCOOH_2]^+$ ions prior to the elemental composition analysis. The parameters for the elemental composition analysis were set as follows unless stated otherwise: (1) tolerance: 25 ppm; (2) DBE (double bond equivalent): minimum 1.5, maximum 4, 5 or 6 depending on if the wax ester was saturated, monounsaturated or diunsaturated; (3) elements used: 0–50 C, 0–100 H, 0–2 O and 0–1 N.

Nomenclature

In the traditional shorthand notation for wax esters, the fatty alcohol precedes the fatty acid and they are connected with a hyphen [9, 10, 12]. Alternatively, the fatty acid precedes the fatty alcohol but they are connected with a slash [6, 17]. For instance, stearyl palmitoleate is represented by 18:0–16:1 or 16:1/18:0. The latter format was adopted in this work. Please note that some studies present a mixed format of wax ester shorthand (e.g., 18:0/16:1 for stearyl palmitoleate) [23] and one needs to keep this in mind when comparing the results from different reports.

Results and Discussion

ESI–MS Analysis of Wax Esters

At a cone voltage of 15 V and a collision energy of 5 eV, the ESI–MS spectra of all the wax ester standards predominantly showed ammoniated molecular peaks but included low intensity sodiated and protonated molecule peaks as well as ammonium and sodium ion linked-dimer peaks (Supplementary Figure S1). When the cone voltage was increased to 50 V, the sodiated and protonated molecular peaks were more intense than the ammoniated molecular peaks (Supplementary Figure S2). These high-intensity molecular peaks made it possible to study the fragmentation pattern of different cation adducts of these wax esters using varying collision energies.

In contrast, for the MS analysis of wax esters in EI, CI or APCI mode, typically many fragment ions are generated while peaks corresponding to the molecular species (molecular ions or cation–adducts of molecules) are very small [8, 9, 11–13, 15], which makes accurate detection and quantitation of wax esters very difficult. The difficulty in detection and quantitation of wax esters acquired in CI and APCI mode is further complicated by the presence of $[M-H]^+$ ions and possibly $M^{+\cdot}$ ions in the spectra of wax esters [13, 15]. These $[M-H]^+$ and $M^{+\cdot}$ ions likely result from hydride ion abstraction and charge transfer [32].

ESI–MS/MS of Saturated Wax Esters

Three saturated wax ester standards, i.e., behenyl palmitate (16:0/22:0), behenyl stearate (18:0/22:0) and palmityl behenate (22:0/16:0), were examined by ESI–MS/MS analysis using collision energies of 5, 10, 20 or 30 eV (Fig. 1 and Supplementary Figures S3–13). At the same collision energy, similar dissociation patterns were observed for the protonated species compared to their ammoniated counterparts (behenyl stearate, Supplementary Figures S3–6; behenyl palmitate, Supplementary Figures S7–9; palmityl behenate, Supplementary Figures S10–12). The patterns changed gradually with increasing collision energies. Across all tested collision energies there was always a predominant peak corresponding to $[RCOOH_2]^+$ while at relatively low collision energies ($\leq$20 eV), a lower intensity peak (with higher signal-to-noise ratio) corresponding to $[R']^+$ was also detected. The relative intensity of this previously reported $[R']^+$ peak [17] was at its highest when using a collision energy of 10 eV (Fig. 1 and Supplementary Figure S13).

In addition to $[RCOOH_2]^+$ and $[R']^+$ peaks, many fragment peaks of substantially lower intensity were observed. The relative intensity of these peaks also differed when collision energies were increased (Supplementary Figure S3). When using collision energies of 5, 10 or 20 eV, we observed a predominant series of fragments, most likely resulting from secondary dissociation of $[R']^+$ ions apparently with a series loss of $(CH_2)_m$ groups ($m \geq 3$). Similar peaks were observed by Fitzgerald *et al.*; however, no tentative assignments were made [17]. When the collision energy was increased to 30 eV, in addition to the $[R'-(CH_2)_m]^+$ ($m \geq 3$) series, several additional series of fragment peaks

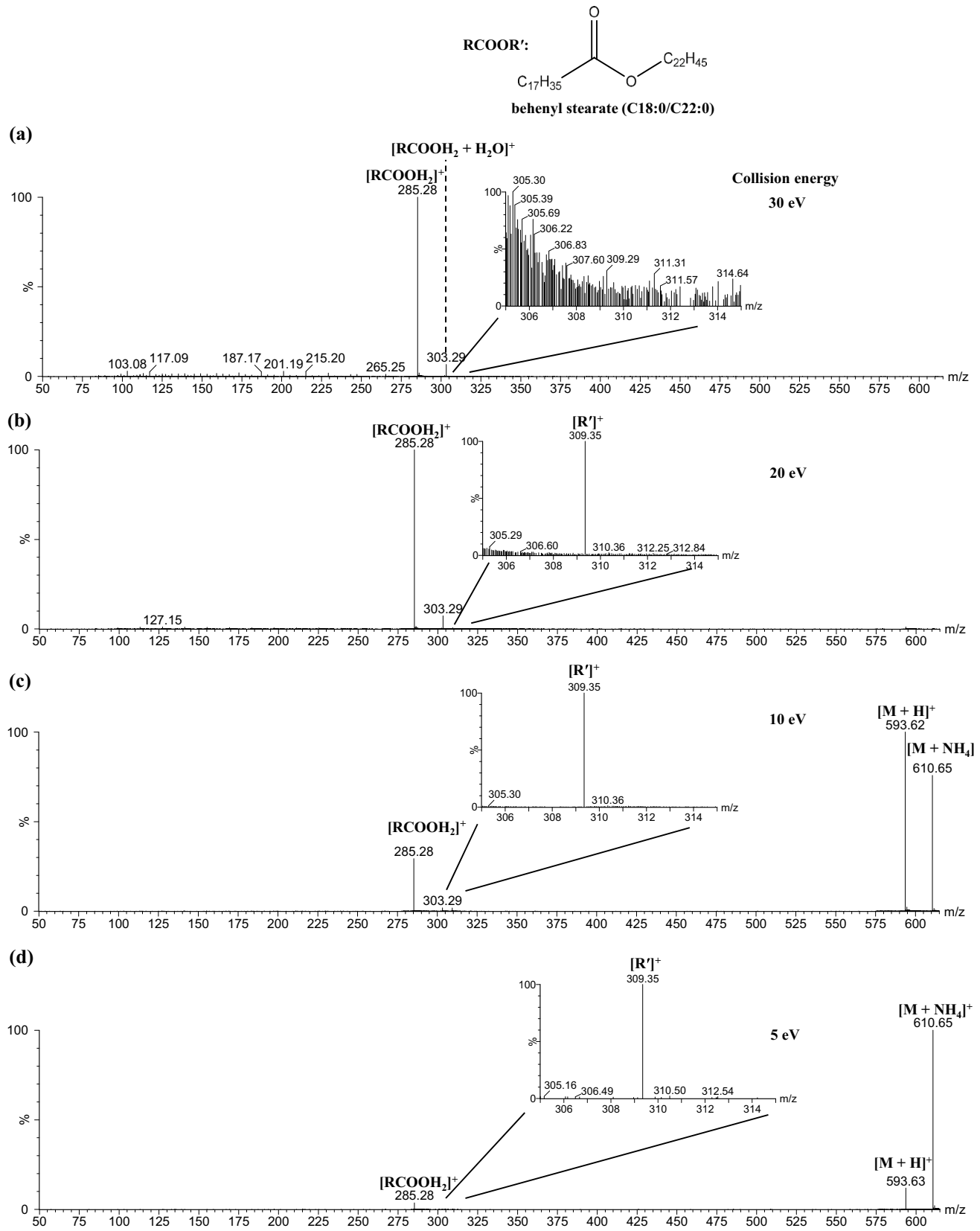

Fig. 1 ESI-CID-MS/MS spectra of the ammonium adduct ion of behenyl stearate (*m/z* 610.65) at collision energies of **a** 30, **b** 20, **c** 10, and **d** 5 eV, respectively

with a difference of CH_2 between the components of each series were observed. The series with the highest intensity peaks likely resulted from secondary dissociation of $[RCOOH_2]^+$ ions and were represented by $[RCOOH_2{-}CH_2{=}CH(CH_2)_{n\text{-}3}CH_3]^+$, or $[RCOOH_2{-}(CH_2)_n]^+$ in simplicity ($n \geq 3$). The same patterns were also observed for the dissociation of other saturated wax ester standards (Supplementary Figures S4-12). The assignments for these series of peaks were supported by pseudo MS^3 analysis of $[RCOOH_2]^+$ and $[R']^+$ peaks (Figs. 2, 3) as well as elemental composition analysis (Supplementary Table S1).

The mechanisms of formation for protonated fatty acids and alkyl ions from dissociation of ammonium/proton adduct ions of wax esters in ESI–MS analysis are likely similar to those proposed for dissociation of some short chain esters (such as alkyl propionates) in chemical ionization MS analysis. The proposed mechanism involves protonation of the ester bond oxygen of the carboxyl group followed by direct cleavage of the alkyl-oxygen bond (for formation of alkyl ions) or with an additional proton transfer from the β carbon to the carbonyl oxygen (for formation of protonated fatty acids) [33]. The charge delocalization on the protonated fatty acid at least partially explains why its intensity was much higher than the alkyl ion.

Interestingly, in each of the MS/MS spectra, peaks corresponding to neutral molecule (including water, methanol and ammonia) adducts of $[RCOOH_2]^+$ ions (Supplementary Figures S4, S6, S7, S9, S10, S12 and S13) were also observed (the corresponding mass errors were less than ± 5 ppm after lock mass correction). The assignments of the water or methanol adducted protonated wax esters were further supported by the pseudo MS^3 spectra (Fig. 2). See "Unusual Adducts Formed between the Direct Product ion $[RCOOH_2]^+$ and the Neutral Molecule in ESI–MS/MS Analysis" for more detailed discussion.

ESI–MS/MS of Wax Esters with Unsaturated Fatty Acid Moieties

For unsaturated wax esters with a double bond in the fatty acid moiety, four wax ester standards, i.e., behenyl palmitoleate (16:1/22:0), behenyl oleate (18:1/22:0), arachidyl oleate (18:1/20:0) and stearyl oleate (18:1/18:0), were examined by ESI–MS/MS analysis using collision energies of 5, 10, 20 or 30 eV (Fig. 4 and Supplementary Figures S14–27). The fragmentation patterns of these unsaturated wax esters were influenced by the collision energy (Fig. 4 and Supplementary Figures S14–26). When using the same collision energy, similar dissociation patterns were observed for protonated wax esters compared to their ammoniated counterparts (Supplementary Figures S15–26). Unlike saturated wax esters which exhibited one predominant fragment peak $[RCOOH_2]^+$ after dissociation (Fig. 1), unsaturated wax esters with a double bond in the fatty acid moiety dissociated into three major peaks that corresponded to $[RCOOH_2]^+$, $[RCO]^+$ and $[RCO{-}H_2O]^+$ (Fig. 4 and Supplementary Figures S14–27). When the collision energy was increased from 5 to 30 eV, the intensity of the $[RCOOH_2]^+$ peak decreased, while the intensities of the $[RCO]^+$ and $[RCO{-}H_2O]^+$ peaks increased (Fig. 4 and Supplementary Figures S14–26).

Similar to our observation for saturated wax esters, there were many fragment ions in the low *m/z* region, particularly when using high collision energies (Fig. 4 and Supplementary Figures S14–26). The relative intensities of these peaks were much higher compared to those of saturated wax esters. These peaks appeared to constitute a related series of peaks resulting from secondary dissociation of $[RCOOH_2]^+$, $[RCO]^+$ and $[RCO{-}H_2O]^+$ product ions. The patterns of these series of peaks were collision energy-dependent. At collision energies of 5–20 eV, the series of peaks with the highest intensities corresponded to $[RCOOH_2{-}CH_2{=}CH(CH_2)_{n\text{-}3}CH_3]^+$, or $[RCOOH_2{-}(CH_2)_n]^+$ in simplicity (Fig. 4, Supplementary Figures S14–26). When the collision energy was increased to 30 eV, two other series, i.e. $[RCO{-}CH_2{=}CH(CH_2)_{o\text{-}3}CH_3]^+$ and $[RCO{-}H_2O{-}CH_2{=}CH(CH_2)_{p\text{-}3}CH_3]^+$, or $[RCO{-}(CH_2)_o]^+$ and $[RCO{-}H_2O{-}(CH_2)_p]^+$ in simplicity ($o \geq 3$, $p \geq 3$), respectively, displayed higher intensities (Fig. 4, Supplementary Figures S14–26). Attributing the low *m/z* series of peaks as resulting from dissociation of the three major peaks was supported by elemental composition analysis (Supplementary Table S1) and pseudo MS^3 analysis of $[RCO{-}H_2O]^+$, $[RCO]^+$ (data not shown) and $[RCOOH_2]^+$ (Fig. 3c) using collision energies of 10 or 20 eV. Pseudo MS^3 analysis of $[RCO{-}H_2O]^+$ resulted in one major series of fragment peaks, i.e., $[RCO{-}H_2O{-}CH_2{=}CH(CH_2)_{p\text{-}3}CH_3]^+$ ($p \geq 3$); pseudo MS^3 analysis of $[RCO]^+$ resulted in a fragment peak $[RCO{-}H_2O]^+$, as well as two major series of peaks, i.e., $[RCO{-}CH_2{=}CH(CH_2)_{o\text{-}3}CH_3]^+$ ($o \geq 3$) and $[RCO{-}H_2O{-}CH_2{=}CH(CH_2)_{p\text{-}3}CH_3]^+$ ($p \geq 3$); and consistently, pseudo MS^3 analysis of $[RCOOH_2]^+$ resulted in two fragment peaks $[RCO]^+$ and $[RCO{-}H_2O]^+$, as well as three major series of peaks, i.e., $[RCOOH_2{-}(CH_2)_n]^+$ (when using a lower collision energy of 5 or 10 eV, data not shown), $[RCO{-}CH_2{=}CH(CH_2)_{o\text{-}3}CH_3]^+$ and $[RCO{-}H_2O{-}CH_2{=}CH(CH_2)_{p\text{-}3}CH_3]^+$ (when using a collision energy of 20 eV, Fig. 3c), where $n \geq 3$, $o \geq 3$ and $p \geq 3$.

Interestingly, in addition to the expected $[R']^+$ peaks from dissociation of saturated wax esters, unusual $[R'{-}2H]^+$ peaks were also observed. The $[R'{-}2H]^+$ peaks were more intense than the corresponding $[R']^+$ peak at collision energies of 5 or 10 eV (Fig. 4, Supplementary Figures S14, S17, S20, S21 and S24). When using a collision energy of 20 eV, a peak corresponding to $[R']^+$ was also observed with an intensity comparable to the $[R'{-}2H]^+$ peak. When the collision energy

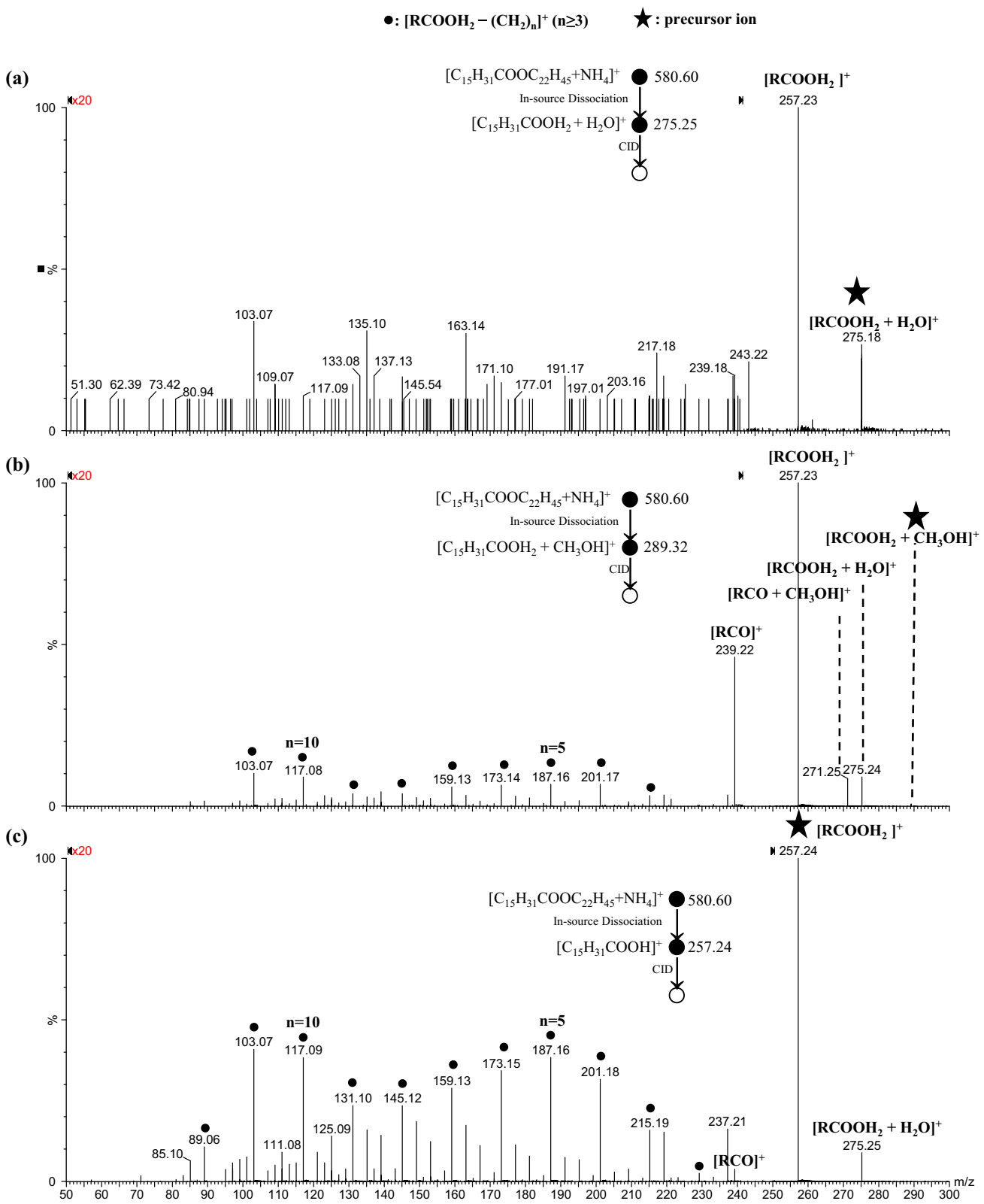

Fig. 2 ESI-CID-MS/MS spectra of product ions that were derived from in-source dissociation of ammonium adduct of behenyl palmitate and ion–molecule interaction: **a** the water adduct of protonated palmitic acid ($[RCOOH_2 + H_2O]^+$), **b** the methanol adduct of protonated palmitic acid ($[RCOOH_2 + CH_3OH]^+$), and **c** the protonated palmitic acid ($[RCOOH_2]^+$). The cone voltage was 75 V and the collision energy was 10 eV. The isolated ions are shown in the figure

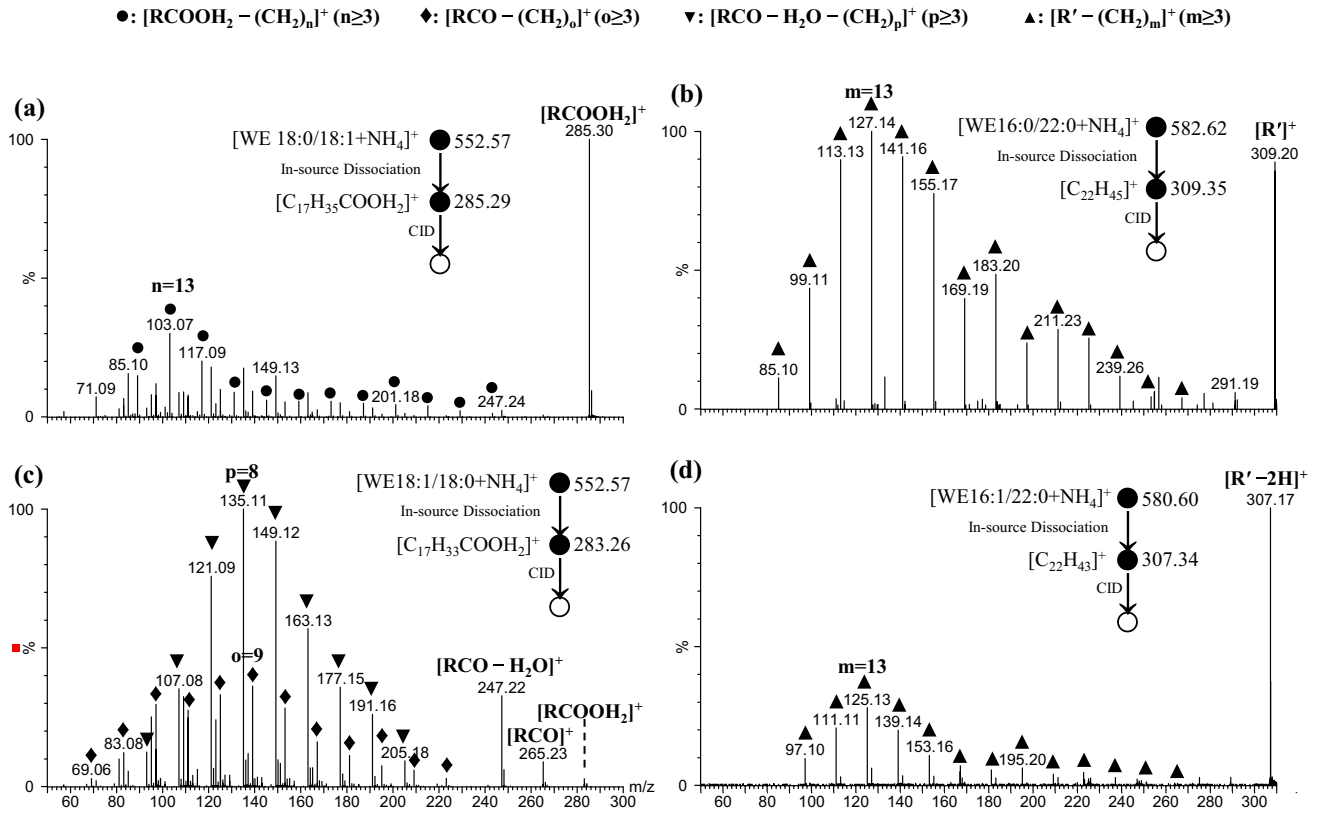

Fig. 3 ESI-CID-MS/MS spectra of product ions that were derived from in-source dissociation of ammonium adducts of oleyl stearate (18:0/18:1), behenyl palmitate (16:0/22:0), stearyl oleate (18:1/18:0), and behenyl palmitoleate (16:1/22:0), respectively: **a** $[C_{17}H_{35}COOH_2]^+$ ($[RCOOH_2]^+$), **b** $[C_{22}H_{45}]^+$ ($[R']^+$), **c** $[C_{17}H_{33}COOH_2]^+$ ($[RCOOH_2]^+$), and **d** $[C_{22}H_{43}]^+$ ($[R'-2H]^+$). The cone voltage was 75 V for **b** and 50 V for other panels; and collision energy was 20 eV for **a** and 10 eV for other panels. The isolated ions are shown in the figure

was increased further, only the $[R']^+$ peak was observed. We propose a formation mechanism for the $[R'-2H]^+$ peak (Supplementary Scheme S1a, see "Unusual Product ions $[R'-2H]^+$ *vs* Product ions $[R']^+$ in ESI–MS/MS Analysis" for detailed discussion). The identity of the $[R'-2H]^+$ peak was supported by pseudo MS^3 analysis (Fig. 3d).

Similar to the MS/MS spectra of saturated wax esters, peaks corresponding to water adduct ($[RCOOH_2 + H_2O]^+$) and ammonia adduct ($[RCOOH_2 + NH_3]^+$ were also observed for ammoniated or protonated forms of these unsaturated fatty acyl-containing wax esters (Supplementary Figures S17, S20, S23 and S26); in contrast, methanol adducts ($[RCOOH_2 + CH_3OH]^+$) were negligible, which could be due to the low intensity of the $[RCOOH_2]^+$ peaks. See "Unusual Adducts formed between the Direct Product ion $[RCOOH_2]^+$ and the Neutral Molecule in ESI–MS/MS Analysis" for more detailed discussion.

ESI–MS/MS of Wax Esters with Unsaturated Fatty Alcohol Moieties

The double bond location in wax esters also significantly affected the fragmentation pattern. When the double bond was in the fatty alcohol moiety instead of the fatty acyl moiety of a wax ester, the fragmentation pattern for the corresponding wax ester significantly changed. Two such wax ester standards, i.e., oleyl stearate (18:0/18:1) and palmitoleyl behenate (22:0/16:1), were examined. Different collision energies were applied for fragmentation of this type of wax ester (Fig. 5, Supplementary Figures S28–34). At low collision energies of 5 or 10 eV, the predominant fragments corresponded to $[R']^+$ and $[RCOOH_2]^+$, although a peak corresponding to $[RCO]^+$ was also observed (Fig. 5, Supplementary Figures S28–35). When the collision energy was increased to 20 eV, the intensity of the peak corresponding to $[R']^+$ decreased substantially while the

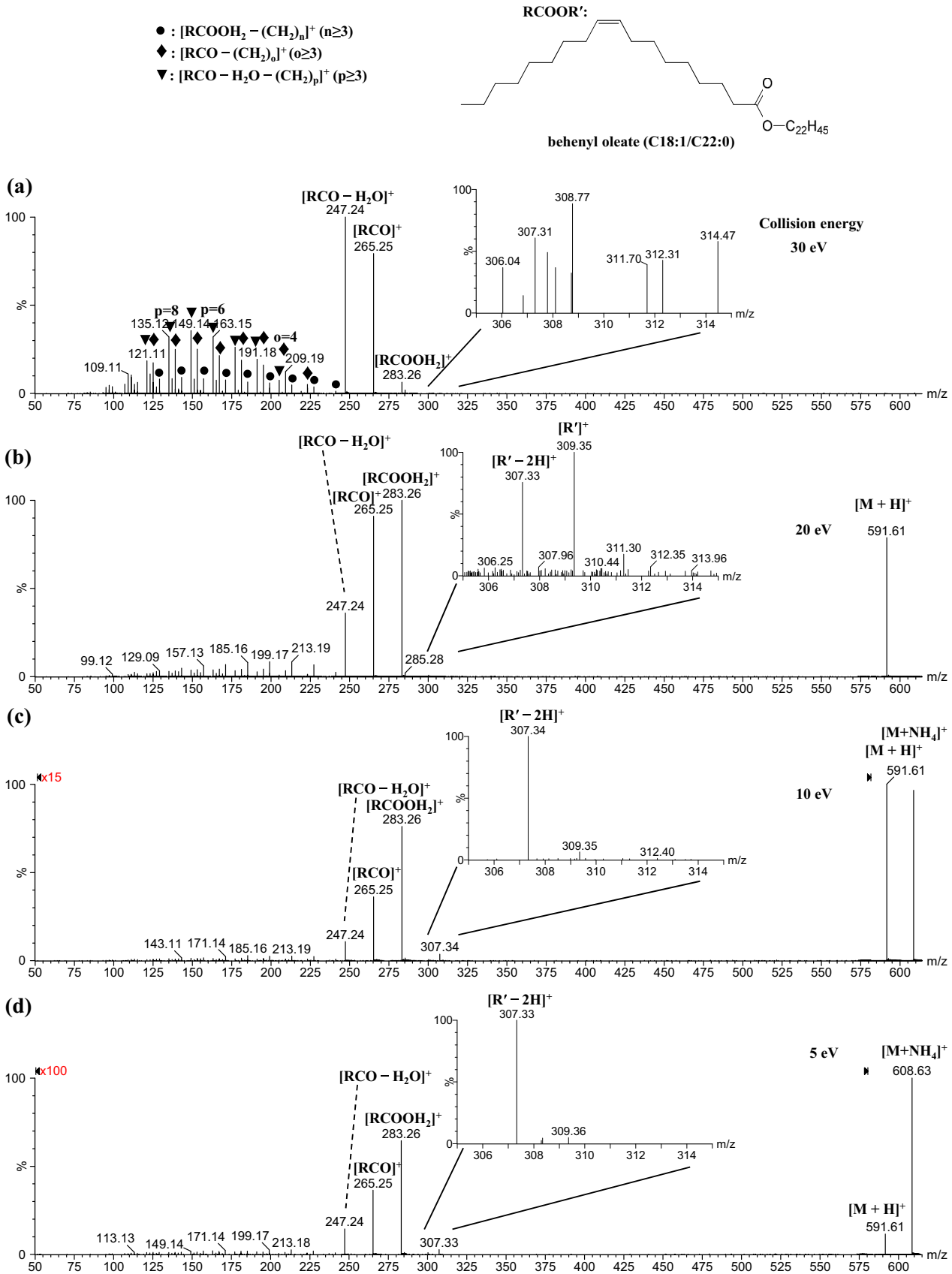

Fig. 4 ESI-CID-MS/MS spectra of the ammonium adduct ion of behenyl oleate (*m/z* 608.63) at collision energies of **a** 30, **b** 20, **c** 10, and **d** 5 eV, respectively

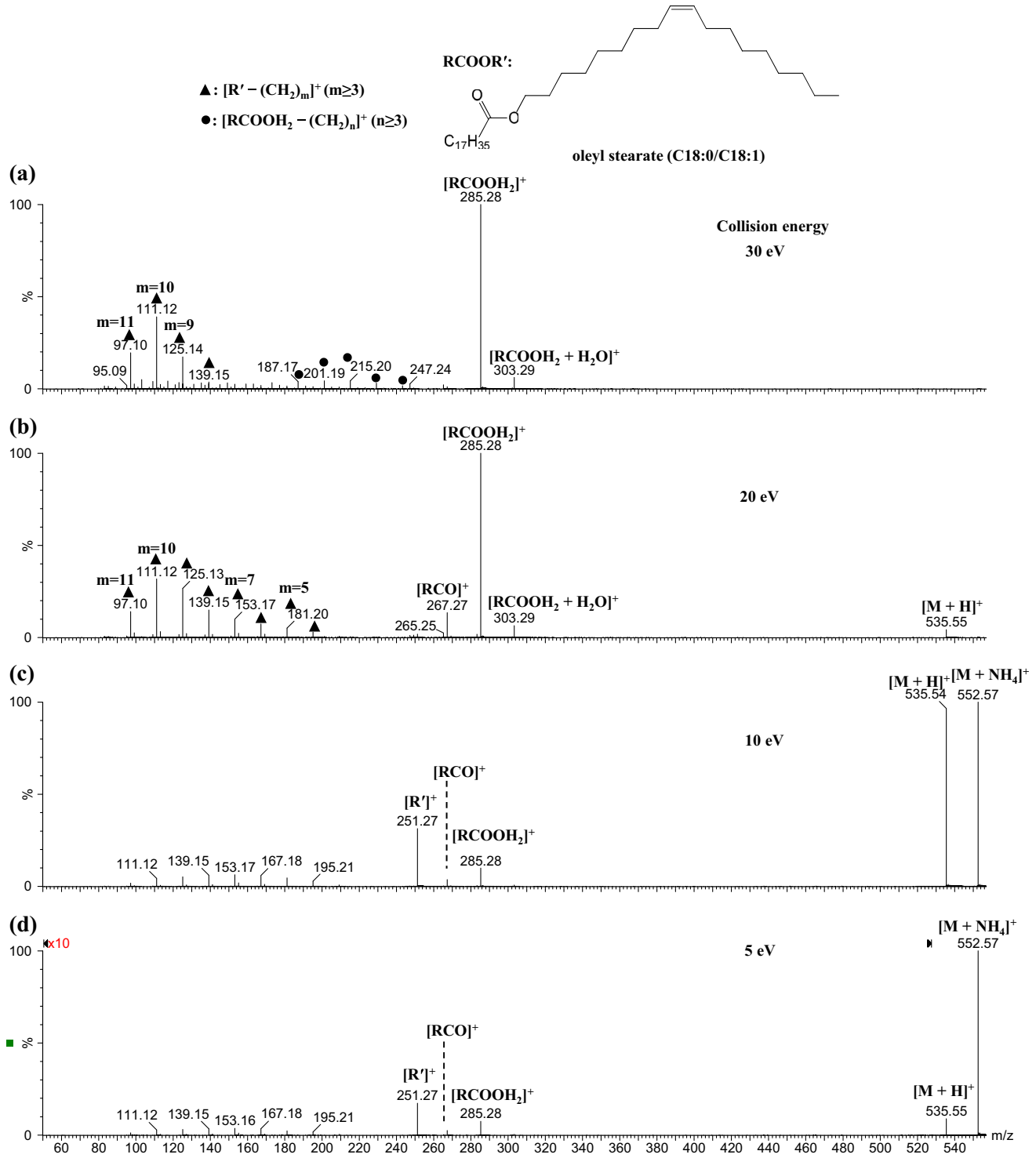

Fig. 5 ESI-CID-MS/MS spectra of the ammonium adduct ion of oleyl stearate (*m/z* 552.57) at collision energy of **a** 30, **b** 20, **c** 10, and **d** 5 eV respectively

intensities of the peaks corresponding to $[RCOOH_2]^+$ and $[RCO]^+$ increased (Fig. 5, Supplementary Figures S28–34). Additionally, when the collision energy was increased to 30 eV, the $[RCOOH_2]^+$ peak was predominant. Regardless of the collision energy applied, the $[RCO-H_2O]^+$ peak was negligible in the MS/MS spectrum of unsaturated wax esters with the double bond in the fatty alcohol moiety (Fig. 5, Supplementary Figures S28–35), which is in

contrast to the observation for unsaturated wax esters with the double bond in the fatty acid moiety (Fig. 4 and Supplementary Figures S14–27).

In the low *m/z* region, the pattern of the fragment peaks for unsaturated fatty alcohol moiety-containing wax esters appeared to be simpler. Compared to several series of fragment peaks for the other type of unsaturated wax esters, there was only one predominant series which corresponded to $[R'-(CH_2)_m]^+$ ($m \geq 3$) (Fig. 5, Supplementary Figures S28–35). This series of peaks was supported by elemental composition analysis (Supplementary Table S1) and pseudo MS^3 analysis of $[R']^+$ (not shown).

Similar to the MS/MS spectra of saturated wax esters, relatively high intensity peaks corresponding to water adduct ($[RCOOH_2 + H_2O]^+$), ammonia adduct ($[RCOOH_2 + NH_3]^+$) and methanol adduct ($[RCOOH_2 + CH_3OH]^+$) were observed from dissociation of ammoniated or protonated forms of these unsaturated fatty alcohol moiety-containing wax esters (Supplementary Table S1, Figures S28, S29, S31, S32 and S34). In contrast, these peaks were smaller for unsaturated fatty acyl-containing wax esters (Supplementary Figures S17, S20, S23 and S26), suggesting that the structure of $[RCOOH_2]^+$ formed from unsaturated fatty acyl-containing wax esters may be different from unsaturated fatty alcohol moiety-containing wax esters. See "Unusual Adducts formed between Direct Product ion $[RCOOH_2]^+$ and Neutral Molecule in ESI–MS/MS Analysis" for a more detailed discussion.

ESI–MS/MS of Wax Esters with Unsaturated Fatty Acid and Fatty Alcohol Moieties

As a representation of wax esters with both moieties unsaturated, oleyl oleate (18:1/18:1) was examined. The fragmentation pattern exhibited characteristics similar to wax esters with either moiety unsaturated. At collision energies of 5 or 10 eV, the major peaks observed corresponded to $[RCOOH_2]^+$, $[RCO]^+$, $[R']^+$ and $[R'-2H]^+$ (Fig. 6 and Supplementary Figures S36–39). When the collision energy was increased, the intensities of the peaks corresponding to $[RCOOH_2]^+$, $[R']^+$ and $[R'-2H]^+$ decreased, while the peaks corresponding to $[RCO]^+$ and $[RCO-H_2O]^+$ as well as those in the low *m/z* region increased (Fig. 6 and Supplementary Figure S36).

Low collision energies of 5 or 10 eV produced a series of peaks in the low *m/z* region resulting from dissociation of R′ (Fig. 6). When the collision energy was increased, the intensities for the other series of peaks increased (Fig. 6). At a collision energy of 30 eV, the following three major series were observed: (1) $[RCOOH_2-CH_2=CH(CH_2)_{n-3}CH_3]^+$, (2) $[RCO-CH_2=CH(CH_2)_{o-3}CH_3]^+$ and (3) $[RCO-H_2O-CH_2=CH(CH_2)_{p-3}CH_3]^+$. These three series can be simplified to (1) $[RCOOH_2-(CH_2)_n]^+$, (2) $[RCO-(CH_2)_o]^+$ and (3) $[RCO-H_2O-(CH_2)_p]^+$ ($n \geq 3$, $o \geq 3$, $p \geq 3$). For the $[R'-(CH_2)_m]^+$ series, three high intensity peaks ($m = 9$, 10 and 11) were present (Fig. 6), like those observed for wax esters with an unsaturated fatty alcohol moiety. The assignment of these series of peaks was supported by elemental composition analysis (Supplementary Table S1) and fragmentation patterns discussed above. It was difficult to unambiguously determine the double bond position from MS/MS analysis, likely due to the migration of a hydride ion [34].

Unusual Adducts Formed Between the Direct Product Ion $[RCOOH_2]^+$ and the Neutral Molecule in ESI–MS/MS Analysis

In the ESI–MS/MS spectra of all examined wax esters (except oleyl oleate), a few peaks corresponding to adducts formed between the neutral molecule (water, ammonia and methanol) and the direct product ion protonated fatty acids ($[RCOOH_2]^+$, derived from dissociation of wax esters) were observed. These neutral molecule adducts include $[RCOOH_2 + H_2O]^+$ (Figs. 1, 5, Supplementary Figures S4, S6, S7, S9–12, S17, S20, S23, S26, S28, S29, S31, S32 and S34), $[RCOOH_2 + NH_3]^+$ (Supplementary Figures S6, S8, S9, S12, S17, S20, S23, S26, S31 and S34) and $[RCOOH_2 + CH_3OH]^+$ (Supplementary Figures S6–9, S12, S17, S20, S23 and S31), although the intensities for the corresponding methanol adducts were much lower. These neutral molecule-product ion adduct peaks were detected with mass errors of typically less than ± 5 ppm after lock mass correction (Supplementary Table S1). Compared to the other wax esters tested, oleyl oleate dissociated most readily, resulting in more fragments and thus making it difficult to detect neutral molecule-product ion adducts (Supplementary Figure S36–39).

The assignment of $[RCOOH_2 + H_2O]^+$ was supported by pseudo MS^3 analysis of $[RCOOH_2]^+$ and $[RCOOH_2 + H_2O]^+$ (Fig. 2): dissociation of $[RCOOH_2 + H_2O]^+$ mainly formed the product ion $[RCOOH_2]^+$, while dissociation of $[RCOOH_2]^+$ formed the product ion $[RCOOH_2 + H_2O]^+$ in addition to a series of product ions corresponding to $[RCOOH_2-(CH_2)_n]^+$ ($n \geq 3$). A similar peak resulting from the dissociation of a wax ester 16:0/16:0 was reported by Fitzgerald *et al.* (Fig. 6a of Ref. [17]). The authors attributed it to an ammoniated carboxylic acid group of an odd electron species [17]; however, their assignment is unlikely as radical ions are not typically formed during ESI–MS analysis of wax esters. A peak corresponding to $[RCOOH_2 + H_2O]^+$ was also apparent in Fig. 3b of Ref. [23].

Interestingly, a number of studies have reported unusual adducts between water and direct product ions derived from a variety of species including guanine [35], guanosine [36, 37], acetophenone [38, 39], halogenated benzoic acids

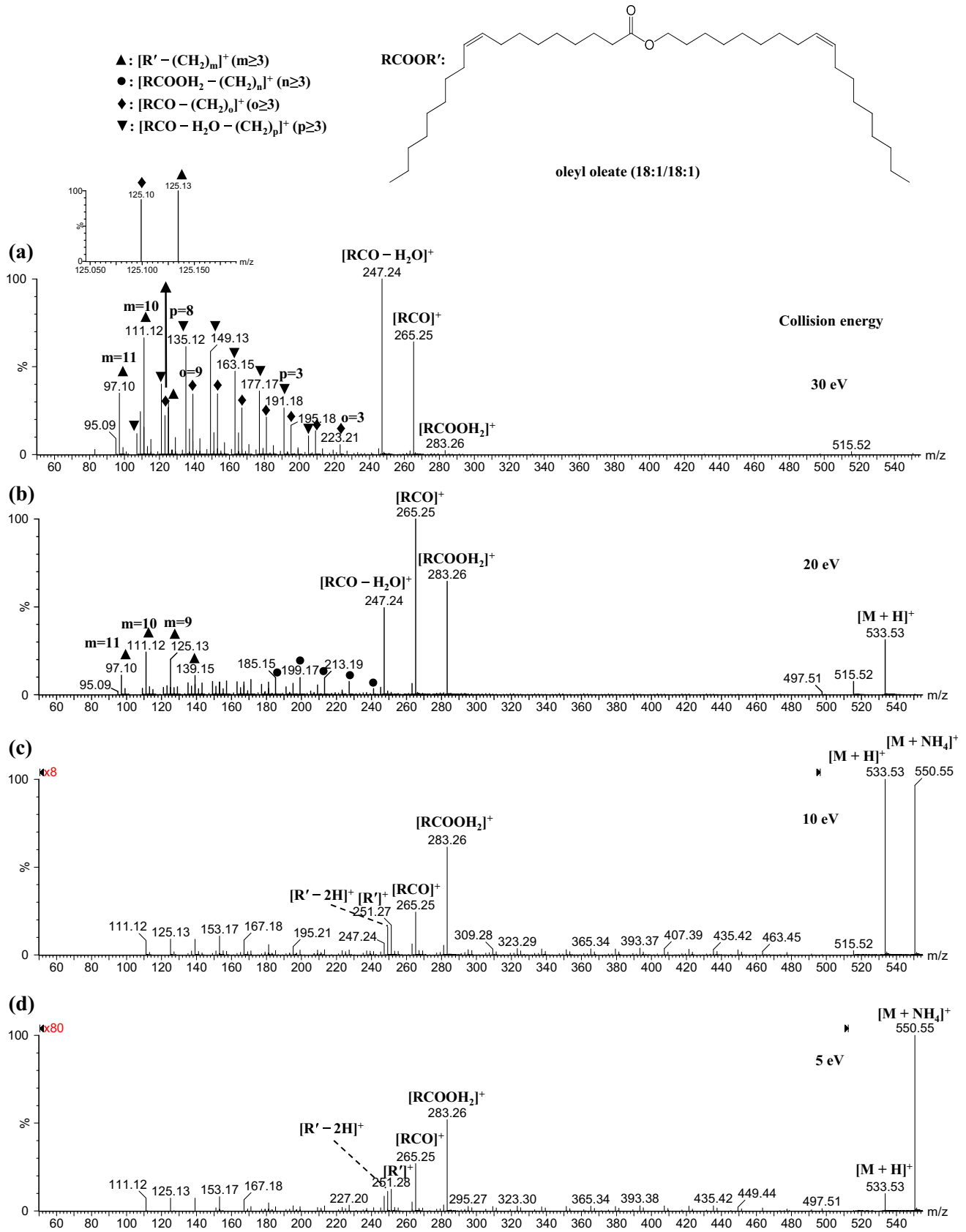

Fig. 6 ESI-CID-MS/MS spectra of the ammonium adduct ion of oleyl oleate (*m/z* 550.55) at collision energies of **a** 30, **b** 20, **c** 10, and **d** 5 eV, respectively

[40], various substituted isoquinoline-3-carboxamides [41] and a series of sulfonic groups–containing ionic liquids [42] in either positive mode [36–39, 41, 42] or negative mode [35, 40]. These water-product ion adducts resulted from ion-water interactions in the collision cell [35–42], where the water molecules were proposed to originate from solvent molecules [36, 42] or being delivered by the collision gas [37, 40]. Similarly, in our study, the water molecule appeared to originate from a combination of solvent and collision gas.

Fragment peaks corresponding to methanol adducts $[RCOOH_2 + CH_3OH]^+$ were also observed. Interestingly, dissociation of $[RCOOH_2 + CH_3OH]^+$ resulted in $[RCOOH_2]^+$ and the unusual product ions $[RCOOH_2 + H_2O]^+$ and $[RCO + CH_3OH]^+$, which corresponded to exchange of CH_3OH with H_2O, and loss of water, respectively (Fig. 2). Adducts between methanol and direct product ions have also been reported in several studies including ESI–MS/MS analysis of guanosine [36] and a series of sulfonic groups-containing ionic liquids [42] as well as APCI-MS/MS analysis of purine and pyrimidine [43]; in addition, two of the studies also reported that MS^3 of the methanol-direct product ion adducts resulted in the loss of methanol or exchange of methanol with water [42, 43].

In addition to the observation of water adducts ($[RCOOH_2 + H_2O]^+$) and methanol adducts ($[RCOOH_2 + CH_3OH]^+$) which have been reported previously, fragment peaks corresponding to ammonia adducts $[RCOOH_2 + NH_3]^+$ were also observed from dissociation of both ammoniated and protonated wax esters. To the best of our knowledge, similar finding have not been reported.

The exact mechanism responsible for the formation of adducts between the neutral molecules and product ions is unclear. However, the absence of the neutral molecule adducts of precursor ions, e.g., $[RCOOR' + H + H_2O]^+$ or $[RCOOR' + NH_4 + H_2O]^+$, suggests that the mechanism involves hydrogen bonding with the carboxylic group of the product ions $[RCOOH_2]^+$. The structures of these neutral molecule adducts including $[RCOOH_2 + H_2O]^+$, $[RCOOH_2 + CH_3OH]^+$ and $[RCOOH_2 + NH_3]^+$ ions were likely in the forms illustrated in Supplementary Scheme S2. Interestingly, the relative intensities of the water adduct peaks were highest when they were derived from saturated wax esters, while lowest when they were derived from wax esters with unsaturated fatty acyl moieties (Figs. 1, 4, 5, and Supplementary Table S2). The difference could be explained by the charge on the carboxyl group being important for the formation of the water adduct (Supplementary Scheme 2): for protonated fatty acids derived from ammonium adducts of saturated wax esters, the carboxyl group was the only charge location; while the charge could be located alternatively on the double bond for protonated fatty acids derived from wax esters with unsaturated fatty acyl moieties. The charge location on the double bond occurs through ammonium adduct formation (or proton adduct formation after loss of ammonia) with the double bond via cation–π interaction [44, 45] and charge-remote dissociation involving a six-membered ring transition state [46, 47] (Supplementary Scheme 1a). The carbon–carbon double bond is a known protonation site in chemical ionization mass spectrometry [48]. The charge on the carboxyl group could have promoted the hydrogen bonding with the water molecule (Supplementary Scheme 2a *vs* 2d).

On the other hand, the relative intensities of the ammonia adduct peaks were higher than those of the water adduct peaks when they were derived from wax esters with unsaturated fatty acyl moieties (Supplementary Figures S17, S20, S23 and S26) compared to when derived from other wax esters (Supplementary Figures S3, S6, S9, S29 and S32). The difference may also be caused by protonation at the carbon–carbon double bond via cation–π interaction [44, 45] rather than the ester bond. This protonation step combined with charge remote dissociation could lead to the formation of protonated fatty acid product ions with the charge located on the double bond instead of the carboxyl group; the location of the charge on the protonated fatty acid in turn resulted in different relative strengths of hydrogen bonding with the neutral molecules (Supplementary Scheme S2e *vs* S2b).

Water adduct formation has been reported to be more common in ion trap mass spectrometers [40]. It would be interesting to see if the formation of adducts between neutral molecule and protonated fatty acids is more pronounced in an ion trap instrument.

Unusual Product Ions $[R'-2H]^+$ *vs* Product Ions $[R']^+$ in ESI–MS/MS Analysis

The typical fragments that contain the fatty alcohol moiety derived from ESI-CID of wax esters were $[R']^+$ ions [15, 17, 23], which most likely resulted from charge-induced dissociation as proposed for short chain esters by Munson *et al*. [33] Interestingly, for dissociation of unsaturated fatty alcohol moiety-containing wax esters, the intensities of the $[R']^+$ peaks were much higher (Fig. 5, Supplementary Figure S35 and Supplementary Table S2), which is reasonably explained by the mechanism we propose that involves the formation of a secondary carbocation (in contrast, a primary carbocation is formed from dissociation of saturated wax esters) and further delocalization of the charge with hydride migration (Supplementary Scheme S1b). Again, the steps include ammonium adduct formation with the double bond via cation–π interaction [44, 45] and charge-remote dissociation involving a six-membered ring transition state [46, 47]. However, more evidence is needed to confirm this mechanism.

The observation of the $[R'-2H]^+$ ions only for unsaturated fatty acyl—containing wax esters was a little surprising (Supplementary Table S2). However, this observation may also result from ammonium adduct formation (or proton adduct after loss of ammonia) with the double bond via cation–π interaction [44, 45] and charge-remote dissociation involving a six-membered ring transition state [46, 47] followed by hydride ion transfer (or a series of sequential transfers) [34, 49] (Supplementary Scheme S1a).

ESI–MS/MS of Sodiated Wax Esters

For sodiated wax esters, the product ions were typically negligible. It is possible that the energy barrier for breaking bonds within wax esters is much higher than the energy barrier for removing the sodium ions from wax esters and thus, the peak corresponding to sodium ion (*m/z* 23) would be the most intense. However, with the mass spectrometer we used, it was difficult to get good detection of this low *m/z* ion.

Tandem Mass Spectra Patterns of Different Types of Wax Esters

The major product ions formed from wax esters depended on the collision energies used for MS/MS. The relative intensities of these product ion peaks were characteristic of different types of wax esters and highest when using a collision energy of 20 eV. At this collision energy, several major product ions were observed for the different types of wax esters: $[RCOOH_2]^+$ for saturated wax esters, $[RCOOH_2]^+$, $[RCO]^+$ and $[RCO-H_2O]^+$ for wax esters with unsaturated fatty acyl moieties, and $[RCOOH_2]^+$ and $[RCO]^+$ for wax esters with unsaturated fatty alcohol moieties. The relative intensities of these ions were also characteristic of different types of wax esters when using a collision energy of 10 eV (Supplementary Table S2). In addition, the different types of wax esters each also produced one or more series of other fragment peaks of different patterns, which may be used to confirm their identities. For instance, at a collision energy 20 eV, the series of peaks observed corresponded to $[R'-(CH_2)_m]^+$ ($m \geq 3$) for wax esters with unsaturated fatty alcohol moieties, $[RCOOH_2-CH_2=CH(CH_2)_{n-3}CH_3]^+$ ($n \geq 3$) mixed with some other series for wax esters with unsaturated fatty acyl moieties, and $[R'-(CH_2)_m]^+$ ($m \geq 3$) for saturated wax esters; additionally, the intensities of these peaks were much lower for saturated wax esters.

Influence of Ionization Modes on Tandem Mass Spectrum Patterns of Wax Esters

When the precursor ions are protonated wax esters, the fragmentation patterns are likely similar whether the ionization mode is CI, APCI or ESI. Indeed, the fragmentation patterns of wax esters in APCI mode reported in Ref. [15] share many similarities with our observations. For example, high intensity $[RCOOH_2]^+$ ions were observed for all wax esters, saturated or unsaturated (regardless of the double bond location); $[RCO]^+$ and $[RCO-H_2O]^+$ ions were observed for the dissociation of wax esters with unsaturated fatty acyl moieties (note wax esters were represented by fatty alcohol moiety–fatty acyl moiety in Ref. [15], while our work referred to them as fatty acyl/fatty alcohol instead); R′ ions were detected from dissociation of both saturated wax esters and wax esters with unsaturated fatty alcohols. However, there were also some differences. One major difference was that Cvacka and colleagues reported a high intensity peak of about 2 Da less than $[RCOOH_2]^+$ for wax ester 20:0/16:1 (they referred to as 16:1–20:0), which was most likely $[RCOO]^+$, along with two high intensity peaks corresponding to the loss of 1 and 2 water molecules from this ion [15]. The major related peaks we observed correspond to $[RCOOH_2]^+$ and $[RCO]^+$. The difference may be caused by the presence of $[M-H]^+$ and $M^{+\cdot}$ ions in addition to the $[M+H]^+$ ion as discussed above for chemical ionization [13, 15]. In addition, the $[R'-2H]^+$ ions observed in our work for wax esters with unsaturated fatty acyl moieties were not reported in Ref. [15], perhaps due to the more gentle ionization technique we used.

Implication for Issues in MRM Quantitation of Wax Esters

Iven *et al*. proposed several possible sources of false positive detection of wax esters by MRM, including matrix-derived background (e.g., steryl esters), untargeted product ions from isobaric wax ester species, and overlapping isotopic peaks of wax esters with different saturation levels [23]. In our work, we report many novel wax ester fragment peaks including those of unexpected (e.g. $[R'-2H]^+$ ions, and adducts with neutral molecules) and under-characterized (e.g., at least four series of peaks $[RCOOH_2-CH_2=CH(CH_2)_{n-3}CH_3]^+$, $[RCO-CH_2=CH(CH_2)_{o-3}CH_3]^+$, $[RCO-H_2O-CH_2=CH(CH_2)_{p-3}CH_3]^+$, $[R'-CH_2=CH(CH_2)_{m-3}CH_3]^+$, where *n*, *o*, *p* or $m \geq 3$) species. These fragment peaks were more complicated when the presence of isotopic distribution was considered. Therefore caution needs to be exercised when using MRM to detect and quantitate wax esters, especially for experiments utilizing direct infusion analysis in the absence of front-end separation. One possible solution for minimizing false positive detection is to use more than one transition for detection of each wax ester species. However, quantitation may still be difficult since the response factor of each transition could be different even for the same precursor ions.

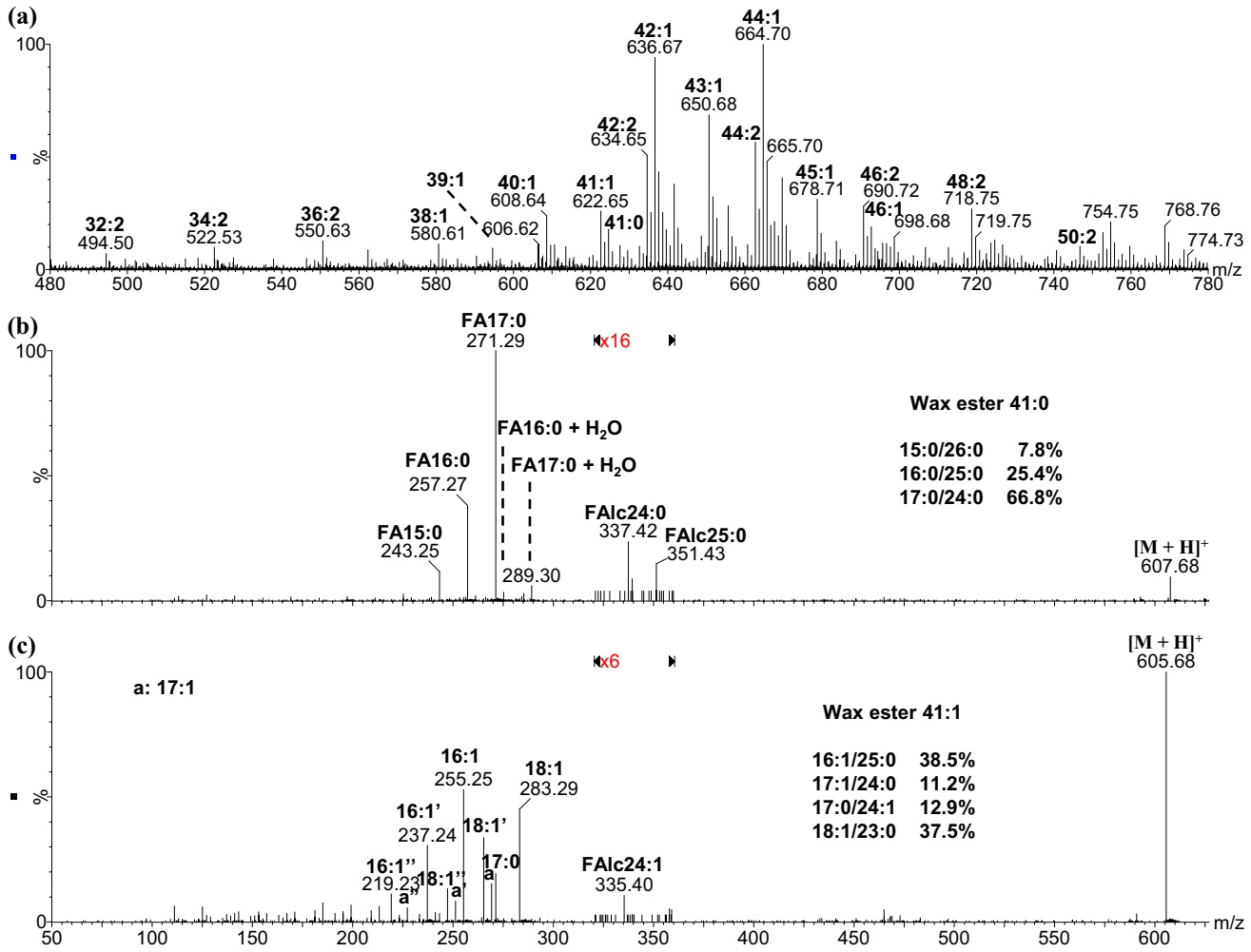

Fig. 7 ESI mass spectrometric analysis of the ammonium adduct ion of wax esters in human meibomian gland secretions: **a** full MS spectrum; MS/MS spectra of **b** wax esters 41:0 (*m/z* 624.67), and **c** wax esters 41:1 (*m/z* 622.65). The cone voltage was 15 V and the collision energy was 20 eV. Major peaks corresponding to wax esters in (**a**), and fatty acid and fatty alcohol moieties in (**b**) and (**c**) were labeled; for convenience, the label "FA" was omitted in (**c**). The water loss peaks and double water loss peaks in (**c**) were indicated with " ' " and " " ", respectively

Applying the Methodology to the Identification of Wax Ester Isomers in Human Meibum

Identification and quantitation of wax esters in human meibum has been reported by our group. [6, 29] However, for each peak of a certain *m/z*, there could be multiple isomers. Dissociation of each peak generated mixed fragments from different isomers. By applying the fragmentation patterns of various types of wax esters, we were able to identify the major isobaric species of each peak. For instance, wax ester 41:0 was actually composed of three major isomers including 15:0/26:0, 16:0/25:0 and 17:0/24:0; while wax ester 41:1 was actually composed of four major isomers including 16:1/25:0, 17:1/24:0, 17:0/24:1 and 18:1/23:0 (Fig. 7). These identifications were supported by the diagnostic product ions of these isomers including $[RCOOH_2]^+$, $[RCO]^+$, $[RCO{-}H_2O]^+$, $[R']^+$ and $[RCOOH_2 + H_2O]^+$. Approximate quantities for the isomers of the wax esters were tentatively determined based on the relative intensity of these diagnostic product ions. A more detailed study is ongoing for in-depth profiling of wax esters in human meibum.

Conclusions

The fragmentation patterns of wax esters depended on several factors. The presence and location (on the fatty acyl moiety or fatty alcohol moiety) of double bonds significantly changed the fragmentation pattern of wax esters. On the other hand, ion–molecule interactions may have formed unexpected product ions due to molecules present in the solvent or delivered by collision gas that were not part of

the precursor ions. The double bond effect and neutral molecule adduct formation observed for dissociation of wax esters could be helpful for identification and quantification of wax esters in biological samples. Current work is ongoing to utilize these fragmentation patterns in conjunction with our earlier work of profiling wax esters in meibum [29] to identify and quantify each isobaric species composition in meibum samples from the corresponding MS/MS spectra. [6].

The formation of the complex between ammonium ion/proton and the carbon–carbon double bond of unsaturated wax esters via cation–π interaction [44, 45] reasonably explains the formation of unusual $[R'-2H]^+$ product ions as well as the relative intensity of neutral molecule adducts (such as $[RCOOH_2 + H_2O]^+$) derived from different types of wax esters. It may also explain the higher ionization efficiency of wax esters and cholesteryl esters with more double bonds [29]. However, to the best of our knowledge, only one such report proposed protonation on the carbon–carbon double bond in chemical ionization mass spectrometry [48]. Consideration of the carbon–carbon double bond as one of the charge adduct sites may help in the interpretation of dissociation mechanisms and ionization efficiencies for other lipid species as well.

Acknowledgments The authors thank NIH for funding (grant number: NEI R01EY015519) and Jeremy Keirsey at the Campus Chemical Instrument Center of the Ohio State University for proofreading and critical comments.

References

1. Tulloch AP (1971) Beeswax—structure of esters and their component hydroxy acids and diols. Chem Phys Lipids 6:235–265
2. Nevenzel JC (1970) Occurrence, function and biosynthesis of wax esters in marine organisms. Lipids 5:308–319
3. Kunst L, Samuels AL (2003) Biosynthesis and secretion of plant cuticular wax. Prog Lipid Res 42:51–80
4. Blomquis GJ, Brakke JW, Byers BA, Jackson LL, Soliday CL (1972) Cuticular lipids of insects. 5. Cuticular wax esters of secondary alcohols from grasshoppers *Melanoplus packardii* and *Melanoplus sanguinipes*. Lipids 7:356–362
5. Smith KR, Thiboutot DM (2008) Sebaceous gland lipids: friend or foe? J Lipid Res 49:271–281
6. Chen JZ, Green-Church KB, Nichols KK (2010) Shotgun lipidomic analysis of human meibomian gland secretions with electrospray ionization tandem mass spectrometry. Invest Ophthalmol Vis Sci 51:6220–6231
7. Nicolaides N, Kaitaranta JK, Rawdah TN, Macy JI, Boswell FM 3rd, Smith RE (1981) Meibomian gland studies: comparison of steer and human lipids. Invest Ophthalmol Vis Sci 20:522–536
8. Ryhage R, Stenhagen E (1959) Mass spectrometric studies. 2. Saturated normal long-chain esters of ethanol and higher alcohols. Arkiv Kemi 14:483–495
9. Aasen AJ, Hofstett Hh, Iyengar BTR, Holman RT (1971) Identification and analysis of wax esters by mass spectrometry. Lipids 6:502–507
10. Spencer GF (1979) Alkoxy-Acyl combinations in the wax esters from winterized sperm whale oil by gas chromatography-mass spectrometry. J Am Oil Chem Soc 56:642–646
11. Vajdi M, Nawar WW (1981) GC-MS analysis of some long-chain esters, ketones and propanediol diesters. J Am Oil Chem Soc 58:106–110
12. Urbanova K, Vrkoslav V, Valterova I, Hakova M, Cvacka J (2012) Structural characterization of wax esters by electron ionization mass spectrometry. J Lipid Res 53:204–213
13. Plattner RD, Spencer GF (1983) Chemical ionization mass-spectrometry of wax esters. Lipids 18:68–73
14. Butovich IA, Uchiyama E, McCulley JP (2007) Lipids of human meibum: mass-spectrometric analysis and structural elucidation. J Lipid Res 48:2220–2235
15. Vrkoslav V, Urbanova K, Cvacka J (2010) Analysis of wax ester molecular species by high performance liquid chromatography/atmospheric pressure chemical ionisation mass spectrometry. J Chromatogr A 1217:4184–4194
16. Chen JZ, Green-Church KB, Nichols KK (2011) Author response: on the presence of (O-acyl)-omega-hydroxy fatty acids and their esters in human meibomian gland secretions. Invest Ophthalmol Vis Sci 52:1894–1895
17. Fitzgerald M, Murphy RC (2007) Electrospray mass spectrometry of human hair wax esters. J Lipid Res 48:1231–1246
18. Santos S, Schreiber L, Graca J (2007) Cuticular waxes from ivy leaves (*Hedera helix L.*): analysis of high-molecular-weight esters. Phytochem Analysis 18:60–69
19. Roberts LD, McCombie G, Titman CM, Griffin JL (2008) A matter of fat: an introduction to lipidomic profiling methods. J Chromatogr B 871:174–181
20. Camera E, Ludovici M, Galante M, Sinagra JL, Picardo M (2010) Comprehensive analysis of the major lipid classes in sebum by rapid resolution high-performance liquid chromatography and electrospray mass spectrometry. J Lipid Res 51:3377–3388
21. Murphy RC, Fitzgerald M, Barkley RM (2008) Neutral lipidomics and mass spectrometry. In: Griffiths WJ (ed) Metabolomics, metabonomics and metabolite profiling. Royal Society of Chemistry, Cambridge
22. Garnier N, Cren-Olive C, Rolando C, Regert M (2002) Characterization of archaeological beeswax by electron ionization and electrospray ionization mass spectrometry. Anal Chem 74:4868–4877
23. Iven T, Herrfurth C, Hornung E, Heilmann M, Hofvander P, Stymne S, Zhu LH, Feussner I (2013) Wax ester profiling of seed oil by nano-electrospray ionization tandem mass spectrometry. Plant Methods 9:24
24. Lam SM, Tong L, Reux B, Lear MJ, Wenk MR, Shui GH (2013) Rapid and sensitive profiling of tear wax ester species using high performance liquid chromatography coupled with tandem mass spectrometry. J Chromatogr A 1308:166–171
25. Brown SH, Kunnen CM, Duchoslav E, Dolla NK, Kelso MJ, Papas EB, Lazon de la Jara P, Willcox MD, Blanksby SJ, Mitchell TW (2013) A comparison of patient matched meibum and tear lipidomes. Invest Ophthalmol Vis Sci 54:7417–7424
26. Yocum AK, Chinnaiyan AM (2009) Current affairs in quantitative targeted proteomics: multiple reaction monitoring-mass spectrometry. Brief Funct Genomic Proteomic 8:145–157
27. Kinsinger CR, Apffel J, Baker M, Bian X, Borchers CH, Bradshaw R, Brusniak MY, Chan DW, Deutsch EW, Domon B, Gorman J, Grimm R, Hancock W, Hermjakob H, Horn D, Hunter C, Kolar P, Kraus HJ, Langen H, Linding R, Moritz RL, Omenn GS, Orlando R, Pandey A, Ping P, Rahbar A, Rivers R, Seymour SL, Simpson RJ, Slotta D, Smith RD, Stein SE, Tabb DL, Tagle D, Yates JR, Rodriguez H (2011) Recommendations for mass spectrometry data quality metrics for open access data (corollary to the Amsterdam principles). J Proteome Res 11:1412–1419

28. Keller BO, Suj J, Young AB, Whittal RM (2008) Interferences and contaminants encountered in modern mass spectrometry. Anal Chim Acta 627:71–81
29. Chen J, Green KB, Nichols KK (2013) Quantitative profiling of major neutral lipid classes in human meibum by direct infusion electrospray ionization mass spectrometry. Invest Ophthalmol Vis Sci 54:5730–5753
30. Ginter JM, Zhou F, Johnston MV (2004) Generating protein sequence tags by combining cone and conventional collision induced dissociation in a quadrupole time-of-flight mass spectrometer. J Am Soc Mass Spectrom 15:1478–1486
31. Chen J, Shiyanov P, Schlager JJ, Green KB (2012) A pseudo MS3 approach for identification of disulfide-bonded proteins: uncommon product ions and database search. J Am Soc Mass Spectrom 23:225–243
32. Carroll DI, Dzidic I, Horning EC, Stillwell RN (1981) Atmospheric-pressure ionization mass-spectrometry. Appl Spectrosc Rev 17:337–406
33. Munson MSB, Field FH (1966) Chemical ionization mass spectrometry. 2. Esters. J Am Chem Soc 88:4337–4345
34. Bouchoux G (2013) From the mobile proton to wandering hydride ion: mechanistic aspects of gas-phase ion chemistry. J Mass Spectrom 48:505–518
35. Sultan J (2008) Collision induced dissociation of deprotonated guanine: fragmentation of pyrimidine ring and water adduct formation. Int J Mass Spectrom 273:58–68
36. Tuytten R, Lemiere F, Esmans EL, Herrebout WA, van der Veken BJ, Dudley E, Newton RP, Witters E (2006) In-source CID of guanosine: gas phase ion-molecule reactions. J Am Soc Mass Spectrom 17:1050–1062
37. Tuytten R, Lemiere F, Van Dongen W, Esmans EL, Witters E, Herrebout W, Van der Veken B, Dudley E, Newton RP (2005) Intriguing mass spectrometric behavior of guanosine under low energy collision-induced dissociation: H_2O adduct formation and gas-phase reactions in the collision cell. J Am Soc Mass Spectrom 16:1904
38. Creaser CS, Wiliamson BL (1996) Ion-molecule reactions of benzoyl ions in a quadrupole ion trap mass spectrometer. J Chem Soc Perk T 2(3):427–433
39. Creaser CS, Williamson BL (1994) Selective gas-phase ion-molecule reactions of the benzoyl ion. J Chem Soc, Chem Commun 14:1677–1678
40. Attygalle AB, Kharbatia N, Bialecki J, Ruzicka J, Svatos A, Stauber EJ (2006) An unexpected ion-molecule adduct in negative-ion collision-induced decomposition ion-trap mass spectra of halogenated benzoic acids. Rapid Commun Mass Spectrom 20:2265–2270
41. Beuck S, Schwabe T, Grimme S, Schlorer N, Kamber M, Schanzer W, Thevis M (2009) Unusual mass spectrometric dissociation pathway of protonated isoquinoline-3-carboxamides due to multiple reversible water adduct formation in the gas phase. J Am Soc Mass Spectrom 20:2034–2048
42. Cao XJ, Yu Y, Ye XM, Mo WM (2009) Solvation in gas-phase reactions of sulfonic groups containing ionic liquids in electrospray ionization quadrupole ion trap mass spectrometry. Eur J Mass Spectrom 15:409–413
43. Frycak P, Huskova R, Adam T, Lemr K (2002) Atmospheric pressure ionization mass spectrometry of purine and pyrimidine markers of inherited metabolic disorders. J Mass Spectrom 37:1242–1248
44. Ma JC, Dougherty DA (1997) The cation-pi interaction. Chem Rev 97:1303–1324
45. Deakyne CA, Meotner M (1985) Unconventional ionic hydrogen-bonds. 2. $NH^+ \cdots \pi$. complexes of onium ions with olefins and benzene-derivatives. J Am Chem Soc 107:474–479
46. Dua S, Bowie JH, Cerda BA, Wesdemiotis C (1998) Search for charge-remote reactions of even-electron organic negative ions in the gas phase. Anions derived from disubstituted adamantanes. J Chem Soc Perk T 2(6):1443–1448
47. Dua S, Bowie JH, Cerda BA, Wesdemiotis C (1998) The facile loss of formic acid from an anion system in which the charged and reacting centres cannot interact. Chem Commun 2:183–184
48. Field FH (1968) Chemical ionization mass spectrometry. 8. Alkenes and alkynes. J Am Chem Soc 90:5649–5656
49. Vrcek IV, Vrcek V, Siehl HU (2002) Quantum chemical study of degenerate hydride shifts in acyclic tertiary carbocations. J Phys Chem A 106:1604–1611